Humans use minimum cost movements in a whole-body task

Lijia Liu[c,b], Dana Ballard[c]

[a] *Department of Computer Science, The University of Texas at Austin, Austin, TX, 78712, US*
[b] *Lead Contact*
[c] *Corresponding Author Email: lijialiu@cs.utexas.edu*

Abstract

Humans have elegant bodies that allow gymnastics, piano playing, and tool use, but understanding how they do this in detail is difficult because their musculoskeletal systems are extraordinarily complicated. Nonetheless, although movements can be very individuated, some common movements like walking and reaching can be stereotypical, with the movement cost a major factor. A recent study has extended these observations by showing that in an arbitrary set of whole-body movements used to trace large-scale closed curves, near-identical posture changes were chosen across different subjects, both in the average trajectories of the body's limbs and in variations within trajectories. The commonality of that result motivates explanations for this generality. One could be that humans also choose trajectories that are economical in energetic cost. To test this hypothesis, we situate the tracing data within a fifty degree of freedom dynamic model of the human skeleton that allows the computation of movement cost. Comparing the model movement cost data from nominal tracings against various perturbed tracings shows that the latter are more energetically expensive, inferring that the original traces were chosen on the basis of minimum cost. Moreover, the computational approach used to establish minimum cost principle suggests a refinement of what is known about cortical movement representations.

Keywords: Posture analysis, whole body movement, virtual tracing, kinematic representation, movement variation costs

Author Summary

Although motor cortical areas have been extensively studied, their basic response properties are still only partially understood, and it remains controversial whether neural activity relates to muscle commands or to abstract movement features. We provide a new perspective of how movements may be resented in the brain by showing that humans chose trajectories with minimum energy cost while accomplishing goal-directed tasks. Furthermore, most of the current neural control studies are experimental. Our computational methodology coupled with a minimum energy principle suggests a refinement of the brain's storage of remembered movements.

1. Introduction

Advances in the speed of computing and novel formulations of the dynamic equations of motion have engendered a new methodology for understanding human movement fundamentals. Large-scale human musculoskeletal models have be built with the objective of understanding human real time goal-oriented behaviors [1, 2]. These newer models linearize the dynamic equations and use feed-forward integrations that are much better conditioned than previous methods.

However, including all the complexity of the human musculoskeletal system, with over 600 muscles controlling a complex skeletal system with over 300 degrees of freedom can be daunting, espicially if the goal is to generate movements as compared to analyze their properties. Moreover, to achieve its control complexity, the brain coordinates several cooperating neural subsystems. In addition to its vast cortical motor memory system, the forebrain coordinates specialized subsystems such as the Basal Ganglia, and Thalamus and Cerebellum in realizing continuous real-time movement [3]. The upshot is that research progress tends to be specialized [4] and there are many open problems [5].

In the face of these challenges, one modeling route is to forego the level of detail that includes muscles and model more abstract versions of the human system that still use multiple degrees of freedom but summarize muscle effects through joint torques. The computation of the dynamics of such multi-jointed systems recently has also experienced significant advances. The foremost of these, use a kinematic plan to directly integrate the dynamic equations. Several different systems exist, such as MuJoCo, Bullet, Havok, ODE and PhysX, but an evaluation by [6] found them roughly comparable in capability, and only MuJoCo [7] has been applied to human modeling.

Thus there is a place for a exclusively human movement based model that could be used to inform laboratory experiments[8], clinical studies e.g [9] and also verify experiments that have only qualitative results[10, 11]. Our human dynamic model has a singular focus on human movement modeling and features a unique approach to integrating the dynamic equations. We have developed a direct dynamics integration method to extract torques from human subjects in real time [12, 13, 14] based on a unifying spring constraint formalism.

Our focus is the principles behind *large-scale arbitrary movements*, particularly with respect to variations between different subjects. Thus we eschew common movements such as reaching and walking [15, 16, 17] and also studies of small-scale grasping movements [18, 19]. Another peripheral issue is for us that that many movement tasks can have objectives that discourage low energetic solutions but can be readily analyzed with decision-making techniques [20, 21, 22, 23] that focus on repeatability; movements are committed to memory with precedence based on the probability of use.

Our experimental setting starts with measuring the kinematics of a movement. The model divides anatomical parts into discrete segments that have their own inertia and are interconnected to other segments by joints that are mostly rotary. Thus a movement can be described as the time course of the coordinates of the joints. The The model's state is indexed by fifty three-dimensional coordinates of a motion capture suit. The time course of these coordinates provides an equivalent representation of a movement's kinematics.

To refer to the kinematics at a specific time we use the term *posture*. Classically, posture classically is used for particular poses such as sitting or standing, but we use it for arbitrary body orientations.

Although computing torques in the inverse dynamics using kinematics is an advance, the study of the kinematics of arbitrary body movements is in itself challenging to study owing to their variation. Bernstein's famous well-known phrase characterizing repeated movements in terms of " repetition without repetition," emphasizes that repeated movements are never exactly the same [24]. However repeated movement variations are never completely random. Informed by task goals, subjects can shape the variations in different parts of the body by co-contracting muscles to achieve desired dynamics in different sections of a trajectory [25]. Thus in looking for regularities in movements one has to deal with both that the trajectories will vary owing to muscle co-contraction and that the amount of co-contraction itself can be modulated throughout the movements.

These variations, we developed specialized aggregation methods for data analysis that extracted similarities of posture sequences in the face of kinematic variations [26]. The task studied had subjects tracing large-scale three dimensional curves in virtual reality that required a series of whole-body movement sequences. Subjects could freely choose their starting posture and also were given no instructions as to how to comport themselves during the tracing process. Their postures were continuously recorded using the motion-capture system.

The main result was that although the locations tracing data exhibits posture variations, both in repeated of a single subject and in trials by different subjects, the average postures show marked regularities in several aspects of the data that was subject to analysis. A t-test between a proximal relative posture and distal relative posture showed that the difference is significant at the 0.0001 level. Also, the variances in the subjects' postures were correlated. If at a point on the curve the variance of a trace calculated from a subject was relatively large, the average of the variance of all the repeated trials from all subjects would be relatively large also.

The obvious inference from all the observed common movements is that energetic cost should be similar and moreover, these observations arise from a minimum cost principle. To test this hypothesis we computed the cost of dynamic models of different subjects' curve traces and compared these results with the cost of tracing under two different perturbations. In one, the trajectories' cost were computed with small perturbations in the model kinematic positions. In the other the original curves that were displaced in five-centimeter increments. The result of both of these comparisons was that the means the energetic cost of were higher than those of the original curve. These results strongly suggest that that movements can be selected on the basis of predicted minimum cost.

The human system has a broad dichotomy into a lateral system, which includes the cortical component commands, and a medial system, which includes the vestibular component commands. Crudely one can think of the lateral sustem as handling predictions and the medial feedback system handling feedback.

Our model also exhibits these two components. The dynamic calculations are good enough to handle the majority of the torques required, but various inaccuracies in the model require a residual torques such as that would be produced by a vestibular system. Our residual system, is unsophisticated as described in the sections section, but it does an essential job in achieving balance.

2. Background

A general principle of human movement is that our nervous system prefers trajectories that are economical in energetic cost [27, 28]. It has been established for decades and has been well studied. For example, in locomotion, there are a number of experiments showing that humans' walking speed [29], step frequency/length [30, 31, 32, 33, 34, 35, 36], and step width [37, 38] are all corresponding with the minimum metabolic cost,e.g., energetic cost exhibits a U-shaped dependence on step frequency while walking at a constant speed and the minimum of the U-shape curve is consistent with the self-selected or preferred walking frequency [17, 34]. Furthermore, new evidences [39, 40, 41] show the nervous system can adapt preferred gaits to minimize energetic cost.

In the past, a common way to address this minimization principle was to conduct experiments comparing walking or running with many other strange and unpractised gaits [42, 43]. Nowadays, there are three commonly used methods to study energy optimization.

The most straightforward and frequently used method is to measure the metabolic cost, e.g., subjects breath through a mouthpiece to measure rates of oxygen consumption (VO2). For example, subjects were required to walk under different circumstances, and the results showed that the metabolic cost was minimum while subjects walked at the condition which was "comfortable" for them [29, 30, 31, 32, 39, 40, 41].

Measure the changes in muscle coactivation and stiffness using Electromyographic (EMG) is considered a common way to reflect metabolic changes. An experiment [44] proved that that subjects' metabolic cost reduced during the learning process of arm reaching tasks, and their muscle activities and coactivation would parallel changes in metabolic power.

The third method is to build a mechanics-based model and determine if the predicted minimum mechanical cost correlates with people's preferences. A basic understanding of trajectory choice can be obtained by calculating energy cost by using minimal dynamic models, such as two-link or three-link arm models [45, 46], inverted pendulum walking models [33, 34, 35, 37], bounce running models [47]. For example, use the inverted pendulum model to predict the optimal step length and compare it with the subjects' real step length. However, most of the experiments used two-dimensional models and studied human part-body motions in the sagittal plane, such as study leg motions using an inverted pendulum model or arm reaching using a 3-link model.

We conducted a whole-body virtual tracing experiment showing that both the movement's posture trajectories and its kinematic variations showed striking commonalities across subjects [26]. One possible principle of explanations for this generality could be that humans choose trajectories that are economical in energetic cost. To prove it, we need to compute the cost of virtual tracing movements. One possible way is to use the VO2 method to measure the metabolic cost or use the EMG to measure the music coactivation and stiffness directly. However, subjects had already worn a VR helmet on their face during the tracing tasks. Besides, motion-capture suits covered their whole body thus there was no exposed skin for EMG electrodes. Another possible way is to build a dynamic model. However, as we mentioned above, those models were built to simulate part of the human body in two-dimensions.

We further searched for methods to build a dynamic bipedal robot by modeling the whole body with a skeleton of rigid segments connected with joints. The simplest bipedal robot uses three links to represent the torso and two legs in the sagittal plane [48, 49]. Five-link biped robots extend the model using two links to represent each leg [50, 51, 52, 53], while seven-link biped robots further extend it by adding feet to it [54, 55]. Those models have three different states: (1) open-linked – one foot on the ground, (2) closed-linked – two feet on the ground, (3) both feet in the air. Each state corresponds to a different set of motion equations. Most researchers use open-linked models [48, 49, 50, 51, 52, 53, 54, 55]. They assumed that once one foot laid to the ground, the other foot would be lifted immediately.

Recently, 3D modeling of biped robots [56, 57] have been developed as well, however, they are still not sophisticated enough compared with a real human body. A real human can be considered as a 21 hierarchical link humanoid robot with 48 degrees of freedom. Furthermore, because the model can have three different states during a continuous motion, such as running, it is hard for an optimization algorithm performing gradient descent for three different sets of equations that happened alternatively. Therefore, The third method described above is also not fitting for our problem: 1) it is too expensive to build a dynamic model with motion equations, 2) it is too hard to use an optimization algorithm to predict the optimal path for a model with three different dynamic states that happened alternatively.

We developed a novel way to compute the energy cost of human movements by building a dynamic human model [58, 13] on the top of a physical engine – Open Dynamic Engine (ODE)[1]. This dynamic human model works as follows:

1. Forward kinematics: it simulates human motion by following the motion capture data
2. Inverse kinematics: it calls the ODE built-in functions to compute the joint angles and joint angular velocities at each frame.
3. Forward dynamics: it simulates human motion based on the computed joint properties.
4. Inverse dynamics: it calls the ODE built-in function to compute the required joint torques.

At each joint, instantaneous power was computed from the product of net joint torque and joint angular velocity. The work performed at each

[1] https://www.ode.org/

joint were determined by numerically integrating the instantaneous powers over the entire tracing task. In this way, given motion capture data, we can compute the energy cost without building a humanoid biped robot with motion equations. The validation of this dynamic model has been proved in the paper [58, 13].

While doing the virtual tracing experiment, subjects could freely choose their starting posture and were given no instructions on how to comport themselves during the tracing process. Therefore, we could consider subjects traced curves under the conditions which were "comfortable" for them. According to the previous experiments [29, 30, 31, 32, 39, 40, 41], the metabolic cost of movements with those trajectories should be the minimum. To prove it, we perturbed the trajectories and computed the energy cost. As expected, the metabolic cost increased more or less.

3. Results

Using the kinematic data from [26], we scaled the dynamic model to each of the nine subjects and had the models trace of the nine curves of variations of difficulty that are shown in Fig. 1. The energy cost of tracing paths showed marked regularities in the following aspects of the data that was subject to analysis:

1. Analysis of the joints' power while tracing path1 across different subjects showed that although the absolute cost of the movements may

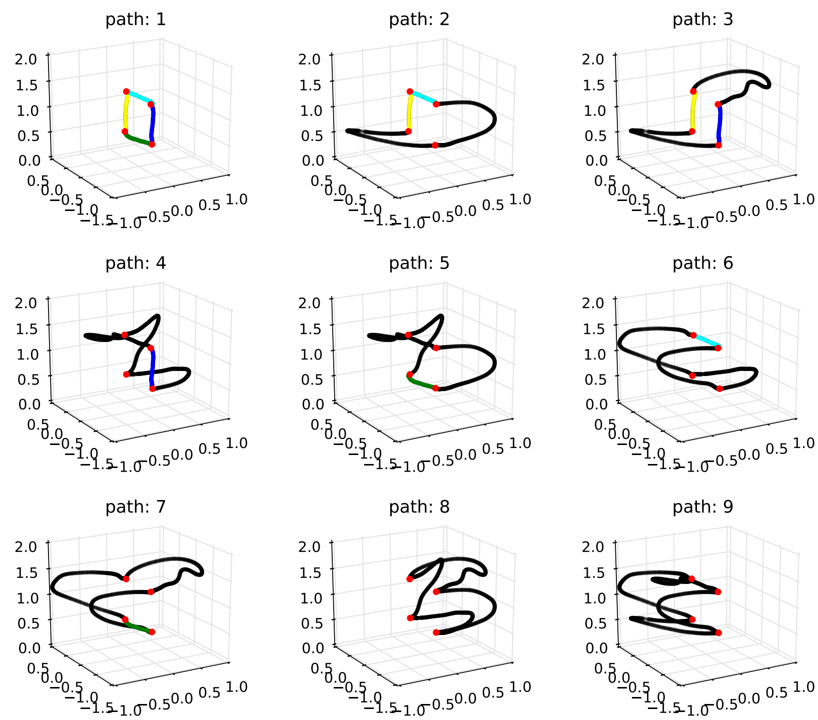

Figure 1: **The nine 3-dimensional paths in the virtual environment that were used in the experiment.** They are ordered by their complexity. For reference, colors denote common segments and points. For the subjects, the paths were all rendered in black, The scale is in meters.

vary between subjects, the cost is qualitatively very similar. (See section 3.1, Figure 2);

2. The computation of average energy cost while tracing path1 showed the corresponding residual forces were relatively small. (See section 3.1, Figure 3 and Figure 4);

3. The costs of tracing each path by each subject, normalized by body weight, are very similar and scaled with the length of the paths. (See section 3.2 and Figure 5);

4. Although there are variations in the cost across the repeated traces, the cost of using the perturbed model parameters is significantly higher than the original. (See See section 3.2, Figure 6 Figure 7, and Figure 8);

5. The increment of energy cost while using perturbed model parameters distributes more on the joints' cost than on the residual component. (See section 3.2 and Figure 9);

3.1. Energy cost analysis of tracing path1

The mean of total power across different participants. As an initial analysis we established the variations in the costs of each curve exhibited by different subjects. A representative result is shown in Fig.2 for path one. The plot shows the total power at each frame for each subject. The trace reveals that the subjects have to put more effort into the trace at the same times. Thus although the absolute cost of the movements may vary between subjects, the costs during the traces are qualitatively very similar. [58] showed different participants used similar postures sequence while tracing the same curves from kinematic perspective. Here, the similarity of the power pattern along frames across different subjects reinforces this conclusion from a dynamics perspective[59].

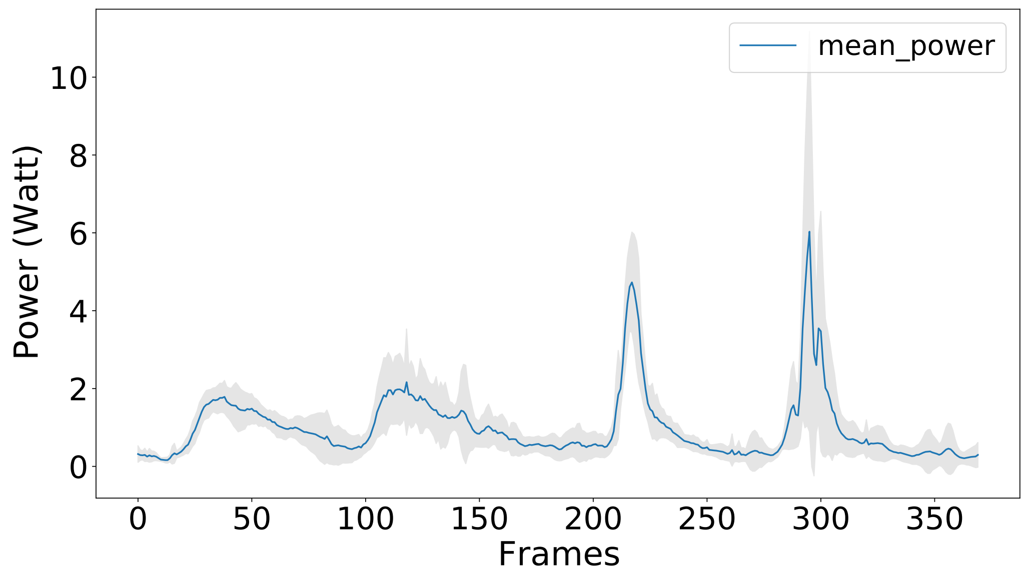

Figure 2: **The mean of power at each frame** Nine subjects traced path1 for 5 times each. The plot shows the joints' power at each frame of different subjects. The small standard deviation means that different subjects had similarity power patterns while tracing the same curve, which shows that the curve has points of difficulty in tracing shared by the subjects. Psth 1 is a simple so it can be traced quickly, but the observation of correlated effort representative of patterns in tracing other curves

Average energy cost of five repetitions. Although there are qualitative similarities in the difficult points on the curve, the totalled costs of the traces differ across different subjects. This result is shown in in Fig. 3, which reports the cost per subject. The total energy of joints including the residual components is shown in blue and the residual component is shown separately in orange. When reporting the costs of the traces, we always use the total cost shown here in blue, which includes the orange residual component.

As shown in Fig. 3, the by far largest cost of the tracing movement is the component owing to the joint torques that are producing the kinetic

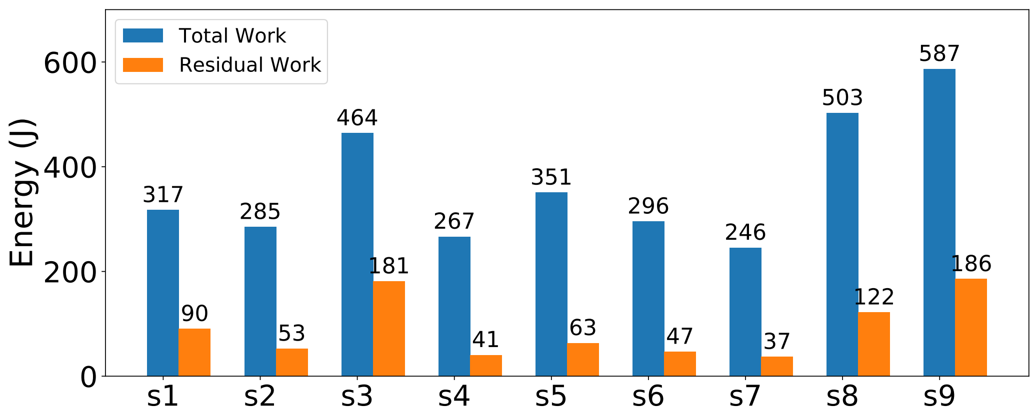

Figure 3: **The average energy cost of tracing and residual force component** Each subject traced path1 with 5 repeats. The horizontal labels indicate the corresponding subjects, e.g. "S1" represents the subject1. The total cost is shown in blue and the portion of that cost due to residual forces is shown in orange, A low cost in residual forces usually signifies that the dynamic model is a good match for that subject's kinematic data.

trajectories, and the additional cost of the residual from the inverse dynamic calculation is small. In the human system, this residual is most prominently due to the vestibular system but just how the vestibular connects to the muscular system is not modeled by the human dynamic model. Instead we implemented a provisional system of torques referred to a coordinate system positioned and the center of mass to maintain balance.

Residual forces. All our subjects' costs are derived from the same inverse dynamics technique [14], which combines measured kinematics and external forces to calculate net joint torques in a rigid body linked segment model. A feature of the dynamic method is that it can reduce potential errors, both in the matches of the motion capture suit and the model. Analogous to

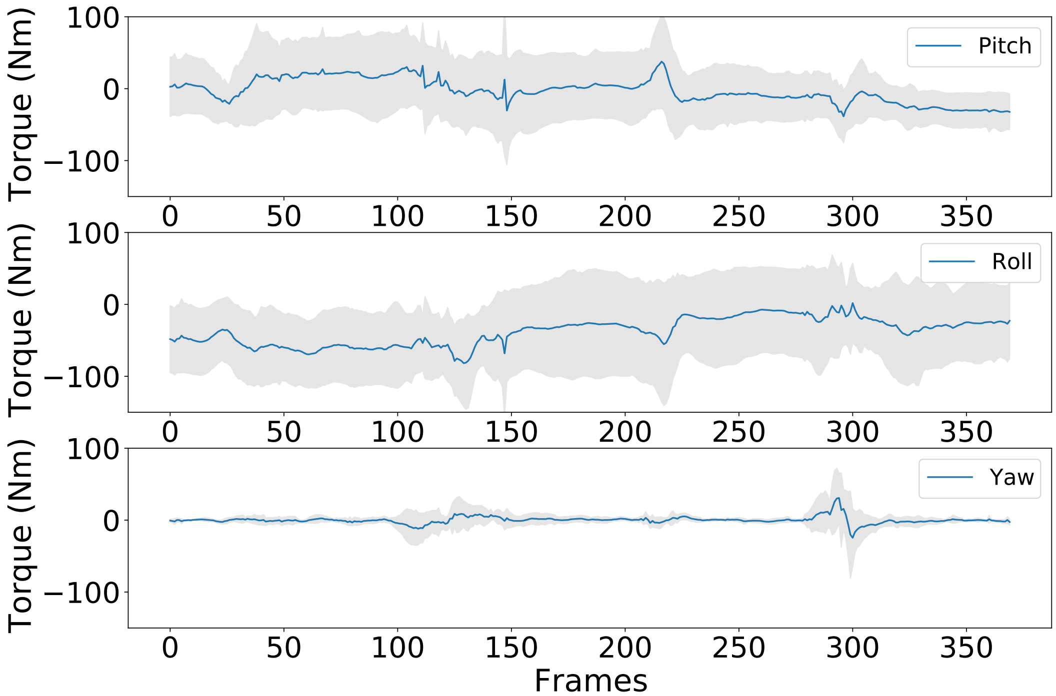

Figure 4: **Residual torque magnitudes**Errors in the calculation of joint torques from the inverse dynamics require additional torques for stabilization. Shown here are the magnitude of the torques seen in pitch roll and yaw axes.)

the human body's ligament structure to join joints, some leeway is allowed in the ,model joints in the integration process.Nonetheless, even after these adjustments, some errors remain. In the model, the main source of the residual forces is usually attributable inaccuracies in the matches between the motion capture suit makers and their match with their corresponding points on the model. This is commonly resolved by introducing 'residual forces' which compensate for this problem . This resolution with a dichotomy of forces is analogous to the human system which combines feed forward lateral pathway forces with medial pathway feedback forces

The temporal cost of such residuals is small as shown in Fig. 4 that shows the distributions of magnitudes of the residual in orange in Fig. 4 for the nine subjects tracing tracing path1. For the model, roll torques are the largest, with pitch torques second. Both pitch and roll torques can exploit the background of the skeleton's inverse pendulum construction for walking. These torques are necessary, but their magnitudes are small and not a factor in distinguishing original and perturbed costs. Residual torques are applied at the figure's waist, which is next to the center of mass. The small magnitudes measured for the residual, together the observation that that the residual is similar for the original and perturbed paths argues against the residual torques being a factor in the analysis.

3.2. Energy cost analysis of tracing individual paths

Energy cost of tracing nine paths. Although there are similar costs per subject in the sample trace, this arrangement does not carry over to the comparison between paths, which has larger differences. We hypothesized that the cost should scale as the length of the path a as shown in Figure 5, which shows the average energetic cost of tracing the nine different paths. The paths differ in tracing cost, but the costs of tracing each path by each subject, normalized by body weight, are very similar and scale with the length of the paths.

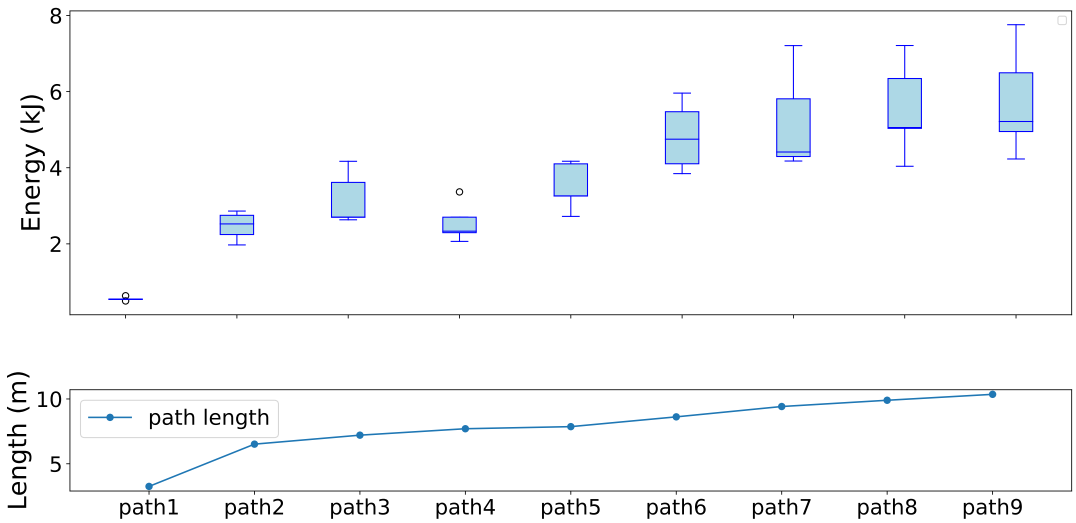

Figure 5: **Cost of tracing** These results portray the possibility that the costs vary across the best-fit five subjects. The statistics show that each path traced has a unique cost that distinguishes it from the rest.

Tracing perturbation. Given these regularities, The next step is to evaluate the significance of perturbations in the tracing protocol. The hypothesis is that if the tracing postures are chosen to be of minimum energy, changing the configuration away from the original tracing situation should incur a cost, and that is what happpens. The first perturbation tests changes in model marker parameters. A marker is changed by a small delta and this is a constraint that is satisfied while the model traces the paths. The way this is implemented is to have the model's right finger follow the cue on the curve as before. The kinematics is as it was for the unperturbed trace, but there is enough freedom so that the dynamics can adapt to follow the perturbed trace.

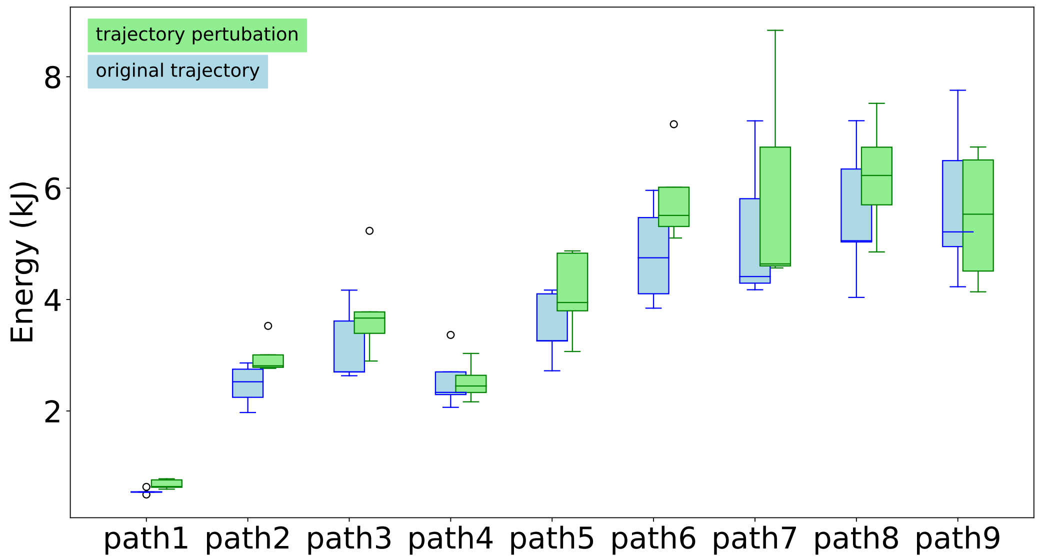

Figure 6: **Cost of tracing perturbed model** Cost of tracing each of the nine paths with a perturbations in the model elbow parameter. The elbow was moved up 3.5cm. This shows that for all the paths and the averages across subject tracers, the original path is always the least expensive. moreover the differences are highly significant

For in each trace the elbow marker is raised by 5 cm. The rest of the system can adapt is the way dictated by the dynamic constraints. The result is shown in Fig.6. Each subject traced each path five times and the resultant costs are averaged. It is seen that although there are variations in the cost across the repeated traces, the cost of using the perturbed model parameters is significantly higher that the original. Note that outside of the changes, the rest of the model solves the inverse dynamic model with the unperturbed parameters, and thus the model has very large degrees of freedom at its proposal.

In the model perturbation experiment, the system must followed the original paths used in the nominal case. The second case makes adjustments in the traced path. Some effects in a displaced can be intuited. For example, if a subject has to reach over their head during the trace, it cam be expected that lowering the traced path would result in a cost savings. For this reason, we chose path perturbations in the horizontal plane. Two such perturbations were used: a 5centimeter dis[placement and a 5 centimeter rightward displacement.

Figure 7 shows the result of averaging the traces across the displaced paths averaged across each subject normalized by body weight. Each original path is seen to be the lowest cost.

Here again the results are striking. Although there is some overlap, for all curves, the originally more economical than the displacements. The observation that the averages of all the perturbed costs are more than the average cost of their original progenitors strongly suggests that energy cost is the factor in the choice of tracing postures. Figure 8 shows that all the three sets of tests are significant to the p=0.01 level.

Given the dynamics dichotomy, a natural question that rises concerns the magnitude of the extra torques in the perturbation cases. Are the extra costs carried by the dynamic model or the residual? This is easily answered by interrogating the simulation, and it turns out that that dynamics models contribution is overwhelming. This is shown in Fig 9.

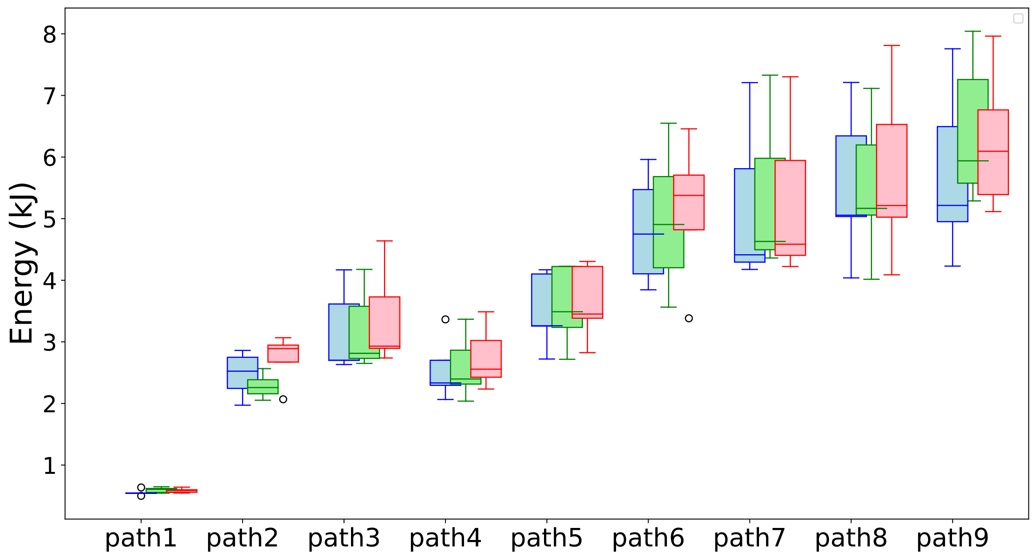

Figure 7: **Cost of tracing perturbed paths** Each of the nine paths have the two perturbations of 5 cm: left in green, right in red. This main result shows that for both averages across subject traces, the original path is always the least expensive.

If the constraints on the dynamics were extremely stiff then the model would have no course other than tracing an exact copy of the unconstrained trajectory and let the residual torques contribute the need difference. However, the markers on the body for these experiments are limited to 15∼18 of key points, leaving the extra degrees of freedom to be determined by the dynamics. Moreover the torque computation, to model the reality of muscles [60] uses uses spring constrains at each joint degree of freedom. Finally the figure is forced to contact the displaced path, and the large features of the movement such as footfalls are the same, leaving the dynamics to fill in the rest.

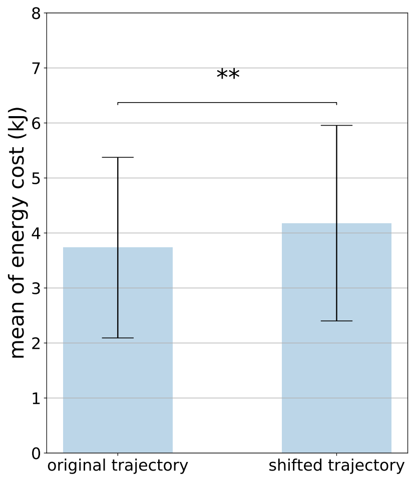

(a) shifted model marker

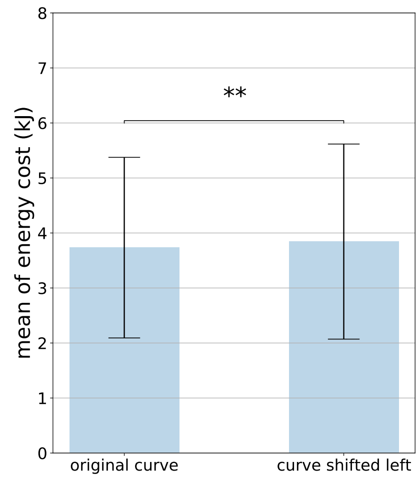

(b) shifted curve (left)

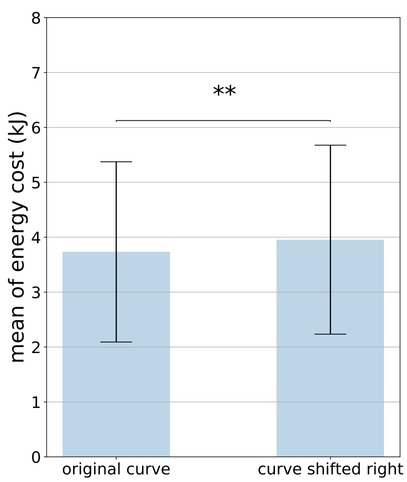

(c) shifted curve (right)

Figure 8: Cost of tracing perturbed paths. Each of the nine paths have three perturbations. (a) Perturbed model marker. (b) curve perturbed 5 cm to the left (b) curve perturbed 5 cm to the right. This main result shows that for both averages across subject traces, the original path is always the least expensive. All three manipulations are different with a significance at the p=0.01 level.

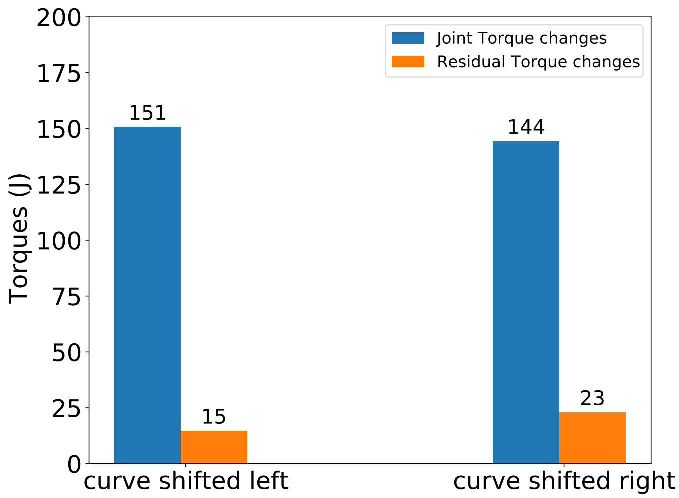

Figure 9: **Extra torques** The extra cost of tracing each of the nine paths with left and right perturbations in the traced path summed over five repeated traces

Discussion

Given that the cost of the movements is are a significant fraction of a human's caloric budget [61] one might expect that humans would exhibit common low cost postures. This turns out to be the case for stereotypical situations such as reaching or walking on a planar surface, but arbitrary whole movements have been less studied so the expectations are more open. Thus it was a surprise to measure arbitrary movements in a large scale tracing task and find markedly common posture sequences used by all tested subjects [26]. An obvious possibility for the similar posture sequences is energetic cost, especially since there were no complex constraints in the movements and no constraints in the time to perform the traces.

Our stimulations extend the kinematic finding to show that tests of human dynamics provide evidence that movements are chosen on the basis of economic energetic costs. The initial measurements were unsurprising. The cost of tracing scales monotonically with the length of a traced path as expected and the necessary residual forces, as would be expected from the human's vestibular system and others, given that the subjects had to choose their movements, were relatively small.

The main substantive results are that subjects' traces of each of nine space paths all have minimal costs with respect to local perturbations. One manipulation introduced perturbations in their kinematic variables. The subjects traced the path but their model with small displacements in kinematic markers. The other experiment used local horizontal displacements of the paths. Vertical were not used as they can be equivocal as the displacements can interact with the different body sizes as when a short subject has to reach up to an uncomfortable height. But outside of this caveat, the all the data can be interpreted as the the tracing posture sequences are selected on the basis of energetic cost.

The hypothesis that humans use minimum cost movement trajectories was tested by the use of a human dynamic model that leverages a major innovation in dynamics computation that allows the the recover torques from kinematic data. The model also provides a fresh perspective for different interpretations of the representations of movements in the brain's motor cortex. The motor cortex has been extensively researched over many decades [62], providing many different perspectives as to its complex structure [63, 64, 65, 66], and the computational modeling cannot be expected to be definitive but it can endorse certain perspectives, which we attempt to do here. The focus is in presenting that our model endorses the use cortical area M1 as the site of kinematics representing posture changes in multiple joints.

Our perspective follows from computer science's classic dichotomy between tables and functions in computation. Computing something as simple as a trigonometric sine function, one has the option of pre-computing sine values at some resolution and memorizing them in a table for instant acess or computing them on line using the slower series expansions for computing the values as needed. These differences are placed in sharper relief in the human system as the on-line aspect is much more formidable owing to the brains relatively slow circuitry. In silicon, processing times are over million faster so the trade-off tends to favor computed functions. In human biology, the vastly slower computations favor pre-computation and tabular formats. the torques for a posture change in an online fashion or pre-compute descriptions ahead of time and save them in memory until needed. The dynamics models advance informs this choice.

These broad computational realities favor memorization, they can also evaluate the different suggestions that have been proposed for motor cortex. The neurobiology of motor cortex also exhibits memorization but also adds another between what we will call *local* and *global* memories. Local memories have been the standard ever since [67] who showed body maps of local movements and somatosensation. Homunculus maps reflect the reality of local stimulation, but eschew any larger picture. The global picture owes its discovery to [68] who show that cortical stimulation could larger posture movements directed to external goals. In this organization the neural maps produce cooperative movements reflective of the animal's task. This organization has been refined by [69]. Using larger amplitude altering current stimulation, Graziano produced large global posture movements that he was able to classify in into five behaviors. A similar point made with very different methodology hasbeen made by [70]. Studies using a balance platform show that humans use muscles is stereo-logical groups.

The global movement data together with the modeling complexity of generating the movements makes it likely that they are pre-computed and save in motor cortex in some form, but what exactly does this take?

The dynamic model argues for parsing the information that can be pre-planned and has reliable generality such as kinematics [71] and stiffness [72]. These parameters are distinguished by having to be pre-planned. Before the movement, many of the details of the movement, such as surface properties are not known and have to be only estimated. Thus the invariant components of the movement are most likely to be memorized.

In contrast, the torques are likely left for the spinal cord. There are many reasons for this. 1) The spinal cord contains a vast store of programmable reflexes that handle the fastest responses. 2 The spinal cord integrates the commands from the brain's lateral system used by the cortex and medial system used by the residual torques like those from the vestibular system.

3) While footfalls can be estimated kinematically, the complex interactions to handle the contact with an uncertain surface need use feedback loops given an kinematic estimate just as a starting point. 4) Given the torques are implied by the kinematics, any manipulation with a kinematic correlate e.g.[73] may have kinematics as its interpretation 5) It has been shown that the extraction of a movement by the cortex has its own dynamic process which is not instantaneous [74], but nonetheless is decoupled with the measure of muscle activation with electromyography. This obversation, together with another that shows supplementary motor cortex is correlated with the timing of movement onset [75], suggest that the motor cortecies, may be focused on the overhead in movement planning than the fine-grained movement dynamics.

4. Methods

4.1. Virtual tracing experiment

For the original kinematic data capture we designed a virtual whole-body tracing experiment to elicit natural movements under common goals [26]. Subjects wore a virtual-reality helmet, Oculus Rift [76], to see a virtual three dimensional interior room with a dojo backdrop via stereo video. They were required to trace a series of paths positioned at fixed locations in the virtual environment. The movements of their bodies and variables relevant to the tasks were simultaneously recorded using the PhaseSpace motion capture system [77]. The WorldViz Vizard software package [78] both controlled the virtual tracing protocol and the recording of the motion capture data. Fig 10 shows the virtual environment setup. Fig 1 shows the nine paths that subjects traced.

Data pos-processing. For some frames the motion capture system is unable to determine the 3-dimensional location of some markers, thus raw motion capture data usually contains some segments of signal loss (dropouts). Dropouts are relatively infrequent in practice but can occur over significant temporal intervals, which makes linear interpolation a poor choice for reconstructing the raw motion capture data. In this experiment, trajectory-based singular value threshold was implemented to reconstruct missing marker data with a minimal impact on its statistical structure. The data for each subject was interpolated using a separate matrix completion model.

In addition to the data interpolation process if a participant did not trace the path successfully, e.g. their index fingers were too far behind the tracing points at a certain frame, or a recording of a tracing trial failed, e.g. too many markers were off during a tracing which leads to a extremely large joint torques, we would consider this tracing invalid and the data would not be used.

4.2. Human dynamic model

To compute the energy cost of subjects tracing paths, we used our human dynamic model [58]. By replaying the virtual tracing experiment's kinematic data, we can compute can the joints' properties, e.g. torques and angles, at

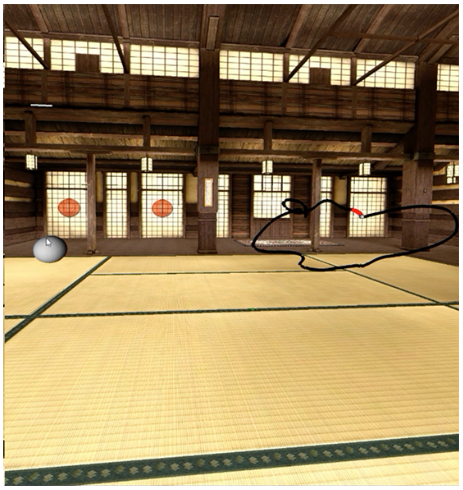

(a) Before tracing

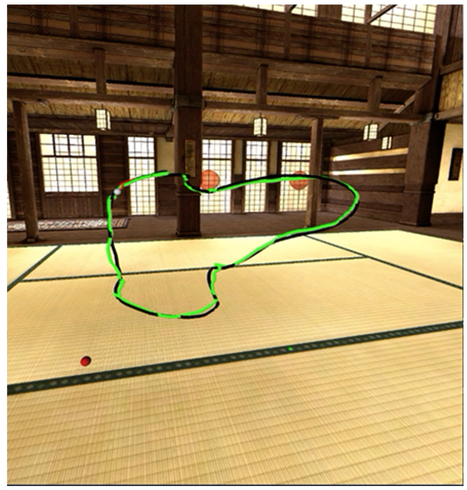

(b) After tracing

(c) A subject doing the tracing task

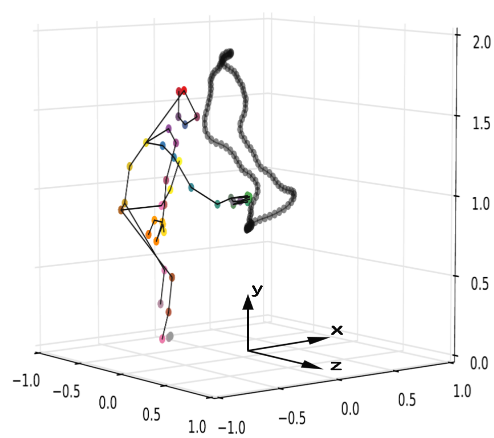

(d) The skeleton plot of the subject

Figure 10: the virtual environment setup. (a) shows a full view of a path, denoted by a black path, and the starting position, denoted by a large white sphere. The small white sphere on the path at the end of a red segment is the tracing target sphere. (b) depicts the scene when a trial is finished. The green path is the actual tracing trajectory generated by a subject. (c) illustrates a subject in the act of tracing a path in the laboratory's motion capture 2 x 2 x 2 meter volume. and (d) shows the lab coordinate system. The scale on the graph is in meters. The the subject's skeleton and the traced path in the 3D space are plotted. The color dots correspond to a subset of the fifty active-pulse LED markers on the suit and the virtual-reality helmet. Related to Figure 2.

frame rates. The human dynamic model is built on top of the ODE physics engine [79]. It consists of a collection of rigid bodies connected by joint. Each joint connects two rigid bodies with anchor points (center of rotation) defined in the reference frame of both bodies. The locations of these anchor points determine the segment dimensions (bone lengths) of the character model. Fig. 11 shows the number of body segments and topology of the human dynamic model.

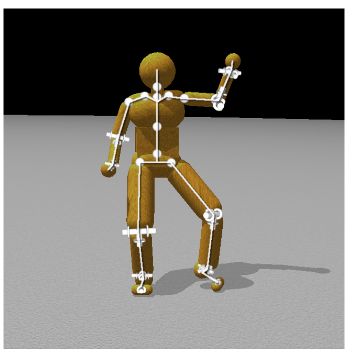

B

Joint	**Part 1**	**Part 2**	**DOF/joint**	Total DOF
Cervical	Head	Neck	3	3
Thoracic	Neck	Upper Torso	3	3
Lumbar	Upper Torso	Lower Torso	3	3
Sacral	Lower Torso	Pelvis	3	3
c.Clavicle	Upper Torso	c.Collar	3	6
c.Shoulder	c.Collar	c.Upper Arm	3	6
c.Elbow	c.Upper Arm	c.Lower Arm	2	4
c.Wrist	c.Lower Arm	c.Hand	2	4
c.Hip	c.Pelvis	c.Upper.Leg	3	6
c.Knee	c.Upper Leg	c.Lower Leg	2	4
c.Ankle	c.Lower Leg	c.Heel	2	4
c.Tarsal	c.Heel	c.Sesamoid	1	2

Figure 11: **The 48 internal DOFModel** A. Four ball-and-socket joints connect five body-segments along the spine from the head to the waist. Ball-and-socket joints are also used at the collar-bone, shoulder, and hip. B. A summary of the joints used in the model. c. = chiral: there are two of each of these joints (left and right). Universal joints are used at the elbows, wrists, knees, and ankles. Hinge joints connect the toes to the heels. All joints limit the range of motion to angles plausible for human movement. Our model assumes that joint DOFs summarize the effects of component muscles.

Fig. 12 shows a interface that allows the simulation of human movements via a multi-purpose graphical interface for analyzing movement data captured through interaction with the virtual environment. With this tool, it is possible to interactively fit a model to motion capture data, dynamically adjust parameters to test different effects, and visualize the results of kinematic and dynamic analysis, such as the example in Fig 13, which shows a four stages in a tracing sequence made originally by a participant of the virtual tracing experiment and recreated by applying the inverse dynamics method using this tool.

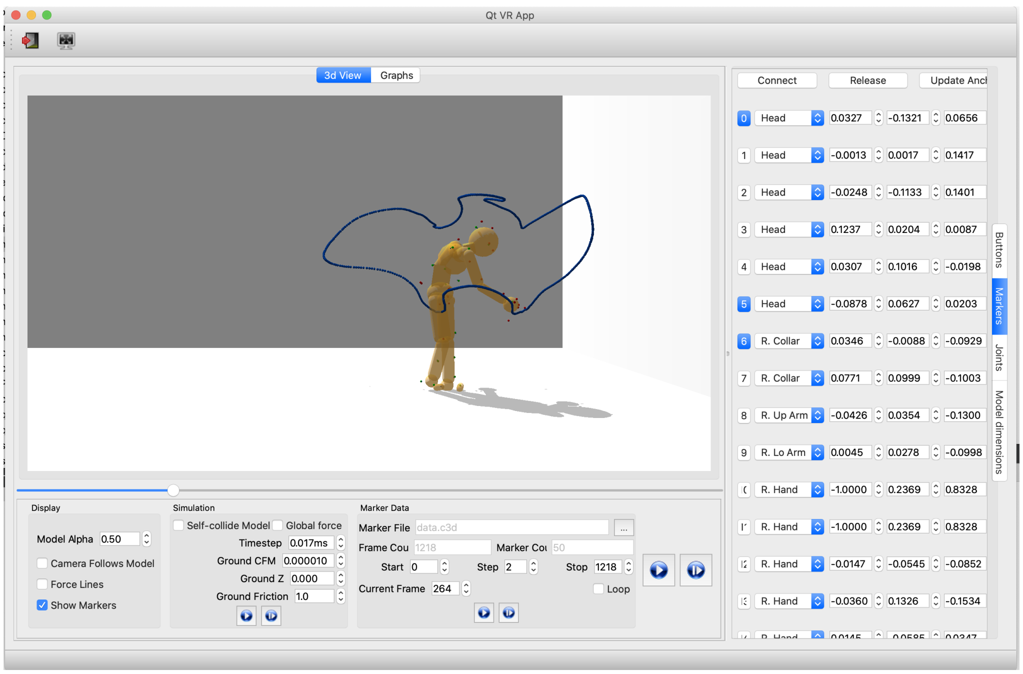

Figure 12: Our analysis tools use the physics engine to compute inverse kinematics and inverse dynamics. They also support various visualizations of relevant data and control for analyzing and producing physically-based movements. The programmed parameters of the model consist of its joints and its 3D marker positions. For example, the right column represents the positions of the markers relative to their corresponding body segments, e.g. the first row shows the information of marker1: 1) "1" represents the marker index, 2) "head" means marker 1 is attaching to the "head" body segment, 3) the remaining three float numbers are marker1's relative position.

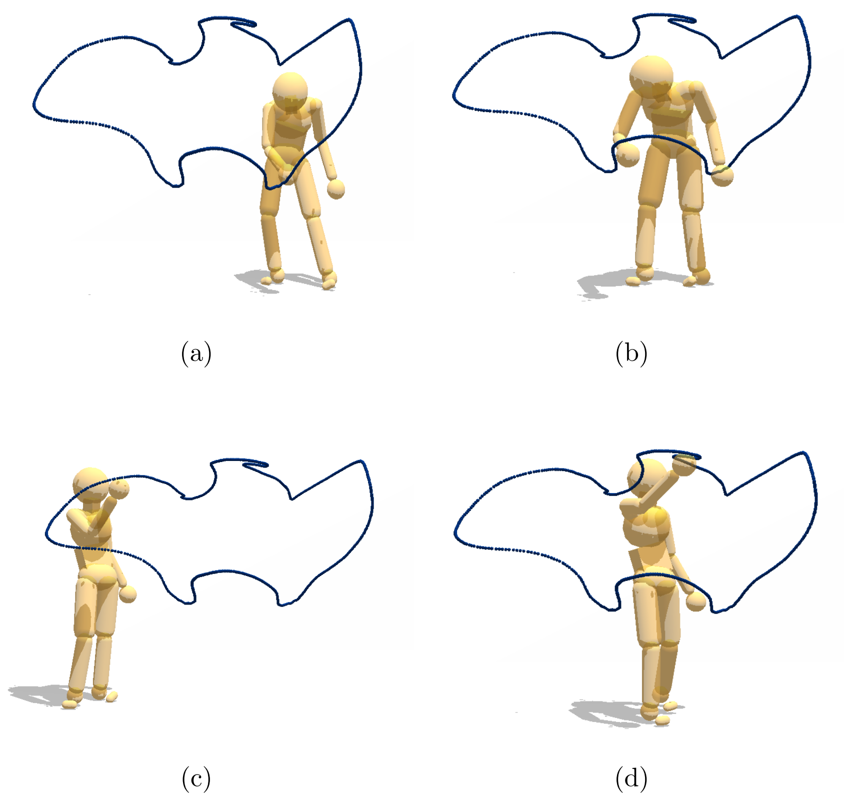

Figure 13: **Model capability illustration.** Four points in a tracing sequence reproduced with physics-engine-based inverse dynamics using recorded motion capture data from a human subject.

Model fitting. The quality of the fit between the data and the model can significantly influence the energy computation. The technique for fitting a model to data begins with a character model that serves as a template, Fig. 12, providing the number of body segments and topology of the model. We further require that labeled markers used in motion capture be assigned to specific model segments. It may be straightforward to derive these using a technique such as in [80, 81]. However, it is also not difficult to do by hand. It would become tedious if one had to go through the process for many different models. Fortunately, the motion capture suit typically puts the markers on the same body segments, even if they are in slightly different places and the body segments have different dimensions.

4.3. Energy cost computation

The centerpiece of the analysis depends critically on the definition of a posture. At each frame, posture is defined as a vector of the joint torques and angles of each of N joints ($N = 22$ in our dynamic human model). The posture p at a frame is a 6n-dimensional column vector presenting the joints properties of the i th participant, thus

$$\mathbf{p} = [\mathbf{j_1}, \mathbf{j_2}, ..., \mathbf{j_N}] \tag{1}$$

$$\mathbf{j_i} = (\boldsymbol{\tau_i}, \mathbf{a_i}) \tag{2}$$

where $\boldsymbol{\tau_i} = (\tau_{i_x}, \tau_{i_y}, \tau_{i_z})$ and $\boldsymbol{a_i} = (a_{i_x}, a_{i_y}, a_{i_z})$ represents the torques and angles of the i th joint at a frame respectively and $i = 1, 2, ..., N$. For the joints whttps://www.overleaf.com/project/5f25a6a28109fa0001d5233chich have less than three dimensions, e.g. hinge joints, universal Joints, the values at unused dimension were assigned zero.

The power W of $i_t h$ joint at a frame t is a scale and equals to the inner product of its torque $\boldsymbol{\tau_i}$ and its angular velocity $\boldsymbol{\omega_i}$, thus

$$\boldsymbol{\omega_i}(t) = \boldsymbol{a_i}(t) - \boldsymbol{a_i}(t-1) \tag{3}$$

$$W_i(t) = \boldsymbol{\tau_i(t)} \cdot \boldsymbol{\omega_i(t)} \tag{4}$$

Therefore the power of a posture at frame t is presented as:

$$W(t) = \sum_{i=1}^{N} W_i(t)$$

Assuming it takes a participant T frames to trace a path, then the total energy cost E of the participant tracing a path is:

$$E = \sum_{t=1}^{T} W(t)$$

The energy cost analysis is naturally organized into three separate stages. Initially, we analyze the subjects energy cost and residual torques of tracing path1 which is the simplest path. Next, we computed the tracing cost of all nine paths. To compare the energy cost of tracing a path across subjects, we computed the average energy cost for all five repeated traces of each subject. Finally, we measured the tracing cost of perturbed participant's trajectories and perturbed paths.

Acknowledgments

This research was supported by National Science Foundation grant CNS1446578 and National Institutes of Health R01 RR09283.

Declaration of Interests

The authors have no financial or personal relationships with other people or organizations that could inappropriately influence their work. The authors declare no competing interests.

References

[1] Delp SL, Anderson FC, Arnold AS, Loan P, Habib A, John CT, et al. OpenSim: open-source software to create and analyze dynamic simulations of movement. IEEE transactions on biomedical engineering. 2007;54(11):1940–1950.

[2] Kidziński Ł, Yang B, Hicks JL, Rajagopal A, Delp SL, Schwartz MH. Deep neural networks enable quantitative movement analysis using single-camera videos. Nature communications. 2020;11(1):1–10.

[3] Shadmehr R, Ahmed AA. Vigor: Neuroeconomics of Movement Control. MIT Press; 2020.

[4] Callahan DM, Umberger BR, Kent-Braun JA. A computational model of torque generation: neural, contractile, metabolic and musculoskeletal components. PloS one. 2013;8(2):e56013.

[5] Loeb GE, Tsianos GA. Major remaining gaps in models of sensorimotor systems. Frontiers in computational neuroscience. 2015;9:70.

[6] Erez T, Tassa Y, Todorov E. Simulation tools for model-based robotics: Comparison of bullet, havok, mujoco, ode and physx. In: 2015 IEEE international conference on robotics and automation (ICRA). IEEE; 2015. p. 4397–4404.

[7] Todorov E, Erez T, Tassa Y. Mujoco: A physics engine for model-based control. In: 2012 IEEE/RSJ International Conference on Intelligent Robots and Systems. IEEE; 2012. p. 5026–5033.

[8] Burk D, Ingram JN, Franklin DW, Shadlen MN, Wolpert DM. Motor effort alters changes of mind in sensorimotor decision making. PloS one. 2014;9(3):e92681.

[9] Kuo AD, Donelan JM. Dynamic principles of gait and their clinical implications. Physical therapy. 2010;90(2):157–174.

[10] Land WM, Rosenbaum DA, Seegelke C, Schack T. Whole-body posture

planning in anticipation of a manual prehension task: Prospective and retrospective effects. Acta psychologica. 2013;144(2):298–307.

[11] Rosenbaum DA, Brach M, Semenov A. Behavioral ecology meets motor behavior: Choosing between walking and reaching paths. Journal of Motor Behavior. 2011;43(2):131–136.

[12] Johnson L, Ballard DH. Efficient codes for inverse dynamics during walking. In: Twenty-Eighth AAAI Conference on Artificial Intelligence. Citeseer; 2014. .

[13] Cooper JL, Ballard D. Realtime, physics-based marker following. In: International Conference on Motion in Games. Springer; 2012. p. 350–361.

[14] Cooper JL. Analysis and synthesis of bipedal humanoid movement: a physical simulation approach. 2013;.

[15] Flash T, Henis E. Arm trajectory modifications during reaching towards visual targets. Journal of cognitive Neuroscience. 1991;3(3):220–230.

[16] Flash T, Hogan N. The coordination of arm movements: an experimentally confirmed mathematical model. Journal of neuroscience. 1985;5(7):1688–1703.

[17] Zarrugh M, Radcliffe C. Predicting metabolic cost of level walking. European Journal of Applied Physiology and Occupational Physiology. 1978;38(3):215–223.

[18] Bongers RM, Zaal FT, Jeannerod M. Hand aperture patterns in prehension. Human movement science. 2012;31(3):487–501.

[19] Smeets JB, Martin J, Brenner E. Similarities between digits' movements in grasping, touching and pushing. Experimental brain research. 2010;203(2):339–346.

[20] Wolpert DM, Ghahramani Z. Computational principles of movement neuroscience. Nature neuroscience. 2000;3(11s):1212.

[21] Ingram JN, Körding KP, Howard IS, Wolpert DM. The statistics of natural hand movements. Experimental brain research. 2008;188(2):223–236.

[22] de Grosbois J, Heath M, Tremblay L. Augmented feedback influences upper limb reaching movement times but does not explain violations of Fitts' Law. Frontiers in psychology. 2015;6:800.

[23] Körding K. Decision theory: what" should" the nervous system do? Science. 2007;318(5850):606–610.

[24] Berstein NA. The Co-ordination and Regulation of Movements. Pergamon Press; 1966.

[25] Latash ML, Scholz JP, Schöner G. Motor control strategies revealed in the structure of motor variability. Exercise and sport sciences reviews. 2002;30(1):26–31.

[26] Liu L, Johnson L, Zohar O, Ballard DH. Humans Use Similar Posture Sequences in a Whole-Body Tracing Task. Iscience. 2019;19:860–871.

[27] Wolpert DM. Computational approaches to motor control. Trends in cognitive sciences. 1997;1(6):209–216.

[28] Todorov E. Optimality principles in sensorimotor control. Nature neuroscience. 2004;7(9):907–915.

[29] Ralston HJ. Energy-speed relation and optimal speed during level walking. Internationale Zeitschrift für Angewandte Physiologie Einschliesslich Arbeitsphysiologie. 1958;17(4):277–283.

[30] Cotes J, Meade F. The energy expenditure and mechanical energy demand in walking. Ergonomics. 1960;3(2):97–119.

[31] Zarrugh M, Todd F, Ralston H. Optimization of energy expenditure during level walking. European journal of applied physiology and occupational physiology. 1974;33(4):293–306.

[32] Cavanagh PR, Williams KR. The effect of stride length variation on oxygen uptake during distance running. Medicine and science in sports and exercise. 1982;14(1):30.

[33] Holt KG, Hamill J, Andres RO. Predicting the minimal energy costs of human walking. Medicine and science in sports and exercise. 1991;23(4):491–498.

[34] Minetti AE, Capelli C, Zamparo P, di Prampero PE, Saibene F. Effects of stride frequency on mechanical power and energy expenditure of walking. Medicine and Science in Sports and Exercise. 1995;27(8):1194–1202.

[35] Donelan JM, Kram R, Kuo AD. Mechanical work for step-to-step transitions is a major determinant of the metabolic cost of human walking. Journal of Experimental Biology. 2002;205(23):3717–3727.

[36] Umberger BR, Martin PE. Mechanical power and efficiency of level walking with different stride rates. Journal of Experimental Biology. 2007;210(18):3255–3265.

[37] Maxwell Donelan J, Kram R, Arthur D K. Mechanical and metabolic determinants of the preferred step width in human walking. Proceedings of the Royal Society of London Series B: Biological Sciences. 2001;268(1480):1985–1992.

[38] Arellano CJ, Kram R. The effects of step width and arm swing on energetic cost and lateral balance during running. Journal of biomechanics. 2011;44(7):1291–1295.

[39] Selinger JC, O'Connor SM, Wong JD, Donelan JM. Humans can continuously optimize energetic cost during walking. Current Biology. 2015;25(18):2452–2456.

[40] Sánchez N, Park S, Finley JM. Evidence of energetic optimization during adaptation differs for metabolic, mechanical, and perceptual estimates of energetic cost. Scientific Reports. 2017;7(1):1–14.

[41] Wong JD, Selinger JC, Donelan JM. Is natural variability in gait sufficient to initiate spontaneous energy optimization in human walking? Journal of neurophysiology. 2019;121(5):1848–1855.

[42] Margaria R. Biomechanics and energetics of muscular exercise. Oxford University Press, USA; 1976.

[43] Hoyt DF, Taylor CR. Gait and the energetics of locomotion in horses. Nature. 1981;292(5820):239–240.

[44] Huang HJ, Kram R, Ahmed AA. Reduction of metabolic cost during motor learning of arm reaching dynamics. Journal of Neuroscience. 2012;32(6):2182–2190.

[45] Thoroughman KA, Shadmehr R. Electromyographic correlates of learning an internal model of reaching movements. Journal of Neuroscience. 1999;19(19):8573–8588.

[46] Franklin DW, Osu R, Burdet E, Kawato M, Milner TE. Adaptation to stable and unstable dynamics achieved by combined impedance control and inverse dynamics model. Journal of neurophysiology. 2003;90(5):3270–3282.

[47] Srinivasan M, Ruina A. Computer optimization of a minimal biped model discovers walking and running. Nature. 2006;439(7072):72–75.

[48] Lee TT. Trajectory planning and control of a 3-link biped robot. In: Proceedings. 1988 IEEE International Conference on Robotics and Automation. IEEE; 1988. p. 820–823.

[49] Čelikovskỳ S, Anderle M. Stable walking gaits for a three-link planar biped robot with two actuators based on the collocated virtual holonomic constraints and the cyclic unactuated variable. IFAC-PapersOnLine. 2018;51(22):378–385.

[50] Mu X, Wu Q. Synthesis of a complete sagittal gait cycle for a five-link biped robot. Robotica. 2003;21(5):581–587.

[51] Mu X, Wu Q. Sagittal gait synthesis for a five-link biped robot. In: Proceedings of the 2004 American Control Conference. vol. 5. IEEE; 2004. p. 4004–4009.

[52] Mu X. Dynamics and Motion Regulation of a Five-link Biped Robot Walking in the sagittal plane. 2005;.

[53] Krishchenko A, Tkachev S, Fetisov D. Planar walking control for a five-link biped robot. Computational Mathematics and Modeling. 2007;18(2):176–191.

[54] Mousavi PN, Bagheri A. Mathematical simulation of a seven link biped

robot on various surfaces and ZMP considerations. Applied Mathematical Modelling. 2007;31(1):18–37.

[55] Bajrami X, Murturi I. Kinematic Model of the seven link biped robot. IJMET. 2017;8(2):454–462.

[56] Grizzle JW, Chevallereau C, Ames AD, Sinnet RW. 3D bipedal robotic walking: models, feedback control, and open problems. IFAC Proceedings Volumes. 2010;43(14):505–532.

[57] Khusainov R, Shimchik I, Afanasyev I, Magid E. 3D modelling of biped robot locomotion with walking primitives approach in simulink environment. In: Informatics in Control, Automation and Robotics 12th International Conference, ICINCO 2015 Colmar, France, July 21-23, 2015 Revised Selected Papers. Springer; 2016. p. 287–304.

[58] Liu L, Cooper JL, Ballard DH. Computational Modeling: Human Dynamic Model. bioRxiv. 2020;Available from: https://www.biorxiv.org/content/early/2020/08/24/2020.08.23.262048.

[59] Squire L, Berg D, Bloom FE, Du Lac S, Ghosh A, Spitzer NC. Fundamental neuroscience. Academic Press; 2012.

[60] Hogan N. The mechanics of multi-joint posture and movement control. Biological cybernetics. 1985;52(5):315–331.

[61] Nelson WL. Physical principles for economies of skilled movements. Biological cybernetics. 1983;46(2):135–147.

[62] Lemon R. An enduring map of the motor cortex. Experimental Physiology. 2008;93(7):798.

[63] Fetz EE. recognizably coded in the activity of single neurons? Behavioral and brain sciences. 1992;p. 154.

[64] Evarts EV. Relation of pyramidal tract activity to force exerted during voluntary movement. Journal of neurophysiology. 1968;31(1):14–27.

[65] Scott SH. Inconvenient truths about neural processing in primary motor cortex. The Journal of physiology. 2008;586(5):1217–1224.

[66] Morrow MM, Pohlmeyer EA, Miller LE. Control of muscle synergies by cortical ensembles. In: Progress in Motor Control. Springer; 2009. p. 179–199.

[67] Penfield W, Boldrey E. Somatic motor and sensory representation in the cerebral cortex of man as studied by electrical stimulation. Brain. 1937;60(4):389–443.

[68] Georgopoulos AP, Schwartz AB, Kettner RE. Neuronal population coding of movement direction. Science. 1986;233(4771):1416–1419.

[69] Graziano MS, Taylor CS, Moore T. Complex movements evoked by microstimulation of precentral cortex. Neuron. 2002;34(5):841–851.

[70] Ting LH, Macpherson JM. A limited set of muscle synergies for

force control during a postural task. Journal of neurophysiology. 2005;93(1):609–613.

[71] Rosenkranz K, Rothwell JC. Modulation of proprioceptive integration in the motor cortex shapes human motor learning. Journal of Neuroscience. 2012;32(26):9000–9006.

[72] Reynolds C, Ashby P. Inhibition in the human motor cortex is reduced just before a voluntary contraction. Neurology. 1999;53(4):730–730.

[73] Kakei S, Hoffman DS, Strick PL. Muscle and movement representations in the primary motor cortex. Science. 1999;285(5436):2136–2139.

[74] Churchland MM, Cunningham JP, Kaufman MT, Ryu SI, Shenoy KV. Cortical preparatory activity: representation of movement or first cog in a dynamical machine? Neuron. 2010;68(3):387–400.

[75] CZimnik AJ, Haro, Churchland MM. Perturbation of Macaque Supplementary Motor Area Produces Context-Independent Changes in the Probability of Movement Initiation. Journl of Neuroscience. 2019;39(17):3217–3233.

[76] Desai PR, Desai PN, Ajmera KD, Mehta K. A review paper on oculus rift-a virtual reality headset. arXiv preprint arXiv:14081173. 2014;.

[77] PhaseSpace I. phaseSpace Motion Capture; 1994. Available from: https://www.phasespace.com/.

[78] WorldViz. Vizard 3 [Computer Software](Version 3). WorldViz Santa Barbara, CA; 2010.

[79] Smith R, et al. Open dynamics engine. 2005;.

[80] Kirk AG, O'Brien JF, Forsyth DA. Skeletal parameter estimation from optical motion capture data. In: 2005 IEEE Computer Society Conference on Computer Vision and Pattern Recognition (CVPR'05). vol. 2. IEEE; 2005. p. 782–788.

[81] De Aguiar E, Theobalt C, Seidel HP. Automatic learning of articulated skeletons from 3d marker trajectories. In: International Symposium on Visual Computing. Springer; 2006. p. 485–494.